ELECTROCHEMICAL PERFORMANCE FOR MXENE-MOS_2 HETEROSTRUCTURE HYBRID ELECTRODE SUPERCAPACITOR IN DIFFERENT AQUEOUS ELECTROLYTES

M.A. Kosnan[1, 4], M.A. Azam[1*], N.E. Safie[2], A. Takasaki[3], M.F. Allim[1]

[1]Fakulti Teknologi dan Kejuruteraan Industri dan Pembuatan,
Universiti Teknikal Malaysia Melaka, Hang Tuah Jaya, 76100
Durian Tunggal, Melaka, Malaysia

[2]Fakulti Teknologi dan Kejuruteraan Elektrik,
Universiti Teknikal Malaysia Melaka, Hang Tuah Jaya,
76100 Durian Tunggal, Melaka, Malaysia

[3]Department of Mechanical Engineering,
Faculty of Science and Engineering,
Otemon Gakuin University, 2-1-15 Nishiai, Ibaraki,
Osaka 567-8502, Japan

[4]Innovative Ecographe Sdn Bhd, No 51, Jalan Platinum 5/2,
Pusat Perdagangan Nilai Impian, 71800, Negeri Sembilan, Malaysia

*Corresponding Author's Email: asyadi@utem.edu.my

Article History: Received 2 July 2025; Revised 15 October 2025; Accepted November 2025

ABSTRACT: Two-dimensional (2D) materials like molybdenum disulfide (MoS_2) are promising for energy storage due to abundant active sites and short ion diffusion paths. However, MoS_2 nanosheets tend to restack, reducing surface area and electrochemical performance. To overcome this, MoS_2 was integrated with MXene, a conductive 2D material, forming a heterostructure composite. X-ray diffraction (XRD) confirmed the crystallinity, Raman identified the structural properties, while FESEM showed uniform MoS_2 distribution on MXene sheets. Electrochemical performance was evaluated in three different aqeuous electrolytes (6M KOH, 1M H_2SO_4, and 0.5M Na_2SO_4) using cyclic voltammetry and galvanostatic charge-discharge tests. Nickel foam and PVDF were used as the current collector and binder, respectively,

contributing to mechanical and electrochemical stability. Specific capacitance og hybrid electrode at scan rate 1mA showcased 6M KOH (80.410 Fg^{-1}) with highest value followed by, 1M H_2SO_4 (1.901 Fg^{-1}), and 0.5M Na_2SO_4 (3.847 Fg^{-1}). These findings underscore MXene's role in enhancing MoS_2 capacitive properties and emphasize the importance of MXene delamination in optimizing supercapacitor electrode performance, while exploring different electrolytes interaction with the hybrid electrode.

KEYWORDS: *MXene/MoS_2 hybrid; heterostructure composite; supercapacitor; specific capacitance; cyclic stability*

1.0 INTRODUCTION

Two-dimensional (2D) materials have garnered significant attention due to their exceptional structural and electrochemical properties, making them promising candidates for next-generation energy storage systems [1]. In the era of Industry 4.0, there is a growing demand for portable, grid-independent energy devices such as supercapacitors. Among various 2D materials, molybdenum disulfide (MoS_2) has emerged as a potential electrode material owing to its abundant adsorption sites and short ion diffusion pathways [2, 3, 4], as shown in Figure 1.

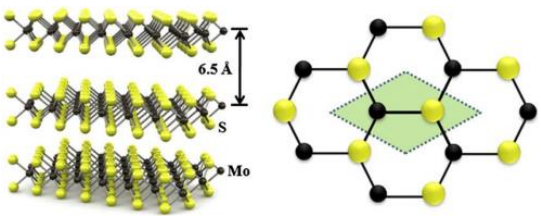

Figure 1 : Atomic structure of MoS_2

However, its practical application is hindered by issues such as layer restacking and volumetric expansion during ion intercalation, which result in capacitance decay and mechanical degradation [4, 5]. To address these limitations, this study proposes the development of a MoS_2/MXene hybrid heterostructure, since heterostructure or hybrid 2D/3D architecture able to avoid layers restacking thus producing increased electroactive area [4, 6] with higher capacitance [7, 8, 9].

Pollack and coworkers also outlined that exploration study on MXene and MoS_2 hybrid materials remain unexplored [10]. MXene is a 2D structure which derived from MAX phase and its composition is Mn+1AXn (n=1,2,3), where M is an early transition metal (M= Ti, Sr, Cr, Ta and etc), A represented the elements mainly from group IIIA and IVA, and lastly X is either C or N (carbon or nitrogen) but it could also be both [4, 5, 8, 9]. MAX is the structure which inter-growing with packed A layers and alternatively stacking of MX layers [5, 6, 9]. It is also known for its excellent electrical conductivity and interlayer tunability, offers a promising platform for enhancing the electrochemical performance of MoS_2-based electrodes [7].

Taking account of considerations above, this project aims to optimize the composition of the MoS_2/MXene hybrid using hydrothermal synthesis and evaluate its electrochemical behavior in various aqueous electrolytes. Comprehensive characterization and electrochemical testing will be conducted to determine the sample with the highest specific capacitance. The synergistic effects between MoS_2 and MXene are anticipated to enhance charge kinetics and structural stability, potentially achieving high specific capacitance with excellent cyclic durability. This work contributes to the development of advanced functional materials for high-performance energy storage applications; the novelty of current study is utilization of heterostructure MoS_2/Ti_3C_2 MXene hybrid electrode in different aqueous electrolytes for supercapacitor applications.

2.0 MATERIAL AND METHODOLOGY

2.1 Synthesis of Ti_3C_2 MXene and MoS_2

To prepare MXene Ti_3C_2, titanium aluminum carbide (Ti_3AlC_2) powder was slowly added into a 40% HF solution and stirred continuously for 24 hours at room temperature. After the reaction, the mixture was washed several times with deionized water and centrifuged at 3500 rpm for 5 minutes until the pH was above 6.0. This step was done to remove the aluminum content. Finally, the sample was dried in a vacuum oven at 50 °C for 12 hours. For MoS_2 preparation, thiourea and ammonium molybdate tetrahydrate ($(NH_4)_6Mo_7O_{24}{\cdot}4H_2O$) were dissolved in deionized water and stirred thoroughly until a uniform solution was formed. The mixture was then transferred into a Teflon-

lined stainless-steel autoclave. The precursor was heated to 210 °C for 40 minutes and maintained at that temperature for 18 hours. After that, the autoclave was allowed to cool naturally to room temperature.

2.2 Synthesis of MoS_2/Ti_3C_2 MXene Hybrid

To prepare the hybrid material of MoS_2 and Ti_3C_2 MXene, as-synthesized MoS_2 powder was combined with an amount gram of Ti_3C_2 MXene powder prepared beforehand in a solution of N-methylpyrrolidone (NMP) in room temperature. This mixture was continuously stirred in range of 800 – 1000 rpm to ensure homogeneity. The resulting solution was then transferred into a Teflon-lined stainless-steel autoclave with a capacity of 28 milliliters. The hydrothermal process was conducted at a temperature of 200 °C under a pressure exceeding 1 atm, with a heating duration of 8 hours. Subsequently, the synthesis process followed the same steps used to prepare pure MoS_2, including the drying phase. After the reaction, the MoS_2/Ti_3C_2 MXene powder was collected for further use. Five different MoS_2:MXene ratios (1:9, 3:7, 5:5, 7:3, and 9:1) were prepared.

2.3 Selection of Current Collector, Binder Type, and Binder Ratio

Selection of a current collector plays a crucial role in determining the overall performance of a supercapacitor. Among the commonly used materials, grafoil paper and nickel foam was chosen due to their distinct structural and electrochemical properties. The electrochemical performance of grafoil paper and nickel foam as current collectors used in supercapacitors were evaluated through CV measurements conducted in a three-electrode setup; where the working, reference and counter electrode are current collector, Ag/Ag+ and platinum wire, respectively. The experiments were performed in a 6 M KOH aqueous electrolyte. The voltage range was set from 0.0 V to 1.0 V with a scan rate of 100 mV/s, selected to assess performance at high scan rates.

Then, the binder selection is critical for ensuring the performance and stability of supercapacitor electrodes. Polytetrafluoroethylene (PTFE) and polyvinylidene fluoride (PVDF) are commonly used binders. In this study, the working electrode was prepared by mixing 80 wt% MoS_2 powder, 10 wt% Super P (TIMCAL) conductive carbon, and 10 wt% binder to form a uniform slurry. This slurry was then coated onto nickel foam with a diameter of 15 mm. The mass loading of the active material

ranged between 0.6 and 1.2 mg. To evaluate structural stability, the prepared samples were immersed in an electrolyte solution for one month.

For binder ratio, optimizing the electrode formulation which in this study, PTFE, can help improve the reliability of the electrodes. The MoS_2 electrodes were prepared based on the compositions listed in Table 1 with binder ratios 5%, 10%, and 20%.

Table 1: Floating-point operations necessary to classify a sample

Sample name	Sample 1 (S1)	Sample 2 (S2)	Sample 3 (S3)
Ratio	MoS_2: AB: PTFE (85:10:5)	MoS_2: AB: PTFE (80:10:10)	MoS_2: AB: PTFE (70:10:20)
Average mass	0.675 mg	0.845 mg	1.29 mg

2.4 Preparation of MoS2/Ti3C2 MXene Hybrid Supercapacitor Electrode

For electrode preparation, PTFE was used as a binder, acetylene black as the conductive agent, N-methylpyrrolidone (NMP) as the solvent, and potassium hydroxide (KOH) as the electrolyte. The electrode slurry was prepared by varying the ratio of active material, binder, and conductive additive according to the experimental design. Once all the samples were prepared, they were mixed and stirred in NMP solvent for at least 5 hours to ensure the slurry was properly mixed and well dispersed. After that, the stirring process continued for another 2–3 hours until a consistent slurry was obtained. The slurry was then coated onto nickel foam, which was used as the current collector, using a simple slurry coating method. The electrodes were then left to dry. The fabrication of the MoS_2/MXene hybrid is carried out via the conventional slurry coating method, where Ti_3C_2 MXene and MoS_2 are dispersed in a suitable solvent to form a uniform slurry. This slurry is then applied onto a substrate to form the electrode.

2.5 Morphological and Structural Characterization

To analyze the structural and morphological properties of pristine and hybrid material, a combination of advanced characterization techniques is employed. These include X-ray Diffraction (XRD) to determine crystallinity and phase composition[Brand: Ringaku

Miniflex Benchtop, 2θ (degree) ranges from 0°-90°, X-Ray Tube: Copper with scan voltage 40 kV] , Raman spectroscopy to assess structural features [Brand: Rigoku, resolution of 0.01 to 0.1o in 2-theta, equipped with a 0.5 to 2.5 Å laser excitation source, 532nm], Field Emission Scanning Electron Microscopy (FESEM) [Brand: HITACHI SU4500, accelerating voltage range of 0.5–30 kV, resolution of the instrument is 1.2 nm at 30 kV and 3.0 nm at 1 kV, with a magnification range of 20x to 800,000x]. Material characterization was carried out using pristine MXene, MoS_2, or the hybrid materials, with or without the addition of conductive agents such as acetylene black.

2.6 Electrochemical Performance Analysis

The electrochemical behavior of the hybrid electrode is evaluated using Cyclic Voltammetry (CV) and Galvanostatic Charge-Discharge (GCD) techniques [WonATech Multichannel Potentiostat/Galvanostat, Model: WMPG1000S]. These methods provide insights into specific capacitance, rate performance, and cyclic stability. Electrochemical measurements are performed in three aqueous electrolytes, such as KOH, NaOH, and H_2SO_4 to assess the ion intercalation behavior and its influence on performance.

Electrochemical evaluations were conducted using a two-electrode system in 6 M KOH electrolyte. CV measurements were performed within a voltage window of 0.0–0.6 V at scan rates of 10, 20, 50, and 100 mV s^{-1}, while GCD measurements were conducted from 0.0–1.0 V at various currents ranging from 0.5 to 2.0 mA. After the CV and GCD analysis were conducted, specific capacitance from each approach will be calculated by using the equation as below:

$$C_{sp} = \frac{A}{mR(V_2 - V_1)} \tag{1}$$

Which (V_2-V_1) = potential window, m= average active mass per electrode, R= scan rates, and A= area under curves. The equation for calculating specific capacitance in the GCD approach is shown below.

$$Specific\ Capacitance\ , C_{sp} = \frac{I \times \Delta t}{m \times \Delta V} = \frac{I_m(\Delta t)}{\Delta V} \tag{2}$$

Which I= current applied, m= average active mass of electrode, Δt =

time difference, I_m= current densities, and ΔV= voltage difference

3.0 RESULTS AND DISCUSSION

3.1 Morphological and Structural Characterization

XRD was used to identify the phases present in MXene, MoS_2, and the hybrid MXene/MoS_2 electrodes. The corresponding XRD patterns are shown in Figure 2 a). The XRD pattern of the exfoliated MoS_2 shows prominent peaks at 2θ angles of 14.6°, 33°, 36.1°, 39.7°, 50°, and 60.6°, corresponding to d-spacing values of 6.07, 2.72, 2.49, 2.27, 1.82, and 1.53 Å. This suggests successful integration of MXene into the MoS_2 structure. Additionally, the absence of a peak near 38°, typically associated with the Al layer in the MAX phase, confirms the effective removal of aluminium during MXene synthesis [5, 8].

Meanwhile, the Raman spectra, as shown in the Figure 2 b), display three distinct profiles corresponding to MoS_2, Ti_3C_2 MXene, and the Ti_3C_2 MXene/MoS_2 hybrid. Each spectrum reflects the characteristic vibrational modes of the respective materials. These features are associated with Ti-C bond vibrations and surface terminations characteristic of MXene materials. The hybrid spectrum combines features from both individual components. It retains the MoS_2 peaks in the 400–450 cm^{-1} range while also exhibiting additional peaks likely associated with MXene or interactions between MoS_2 and MXene.

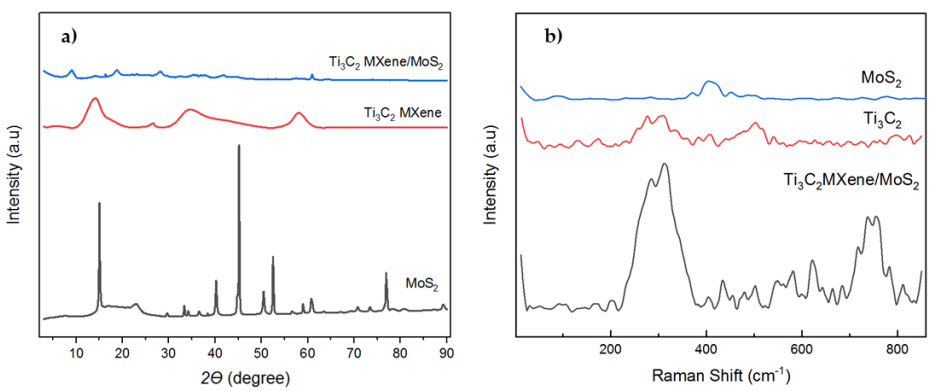

Figure 2: (a) XRD patterns of MoS_2, Ti_3C_2 MXene, and Ti_3C_2/MoS_2; (b) Raman spectra of the sample's study

3.2 Selection of Current Collector, Binder Type, and Binder Ratio

From the three-electrode system, CV analysis conducted for grafoil paper and nickel foam current collector, it was found that CV curves from both current collectors displayed a near-rectangular shape as shown in Figure 3(a) and 3(b); indicative of electric double-layer capacitor (EDLC) behavior. The corresponding data is tabulated in Table 2.

Table 2: C_{sp} results of Grafoil paper and Ni foam in 100 mVs^{-1}

Samples	Area under curves	Scan rates (mVs^{-1})	Average active mass (mg)	Specific Capacitance (Fg^{-1})
Ni foam	0.025627	100	159	1.612
Grafoil	0.001778	100	42	0.4233

In summary, nickel foam demonstrated the highest specific capacitance, with a Csp value of 1.612 F/g, attributed to its low contact resistance and superior EDLC characteristics. Due to its favorable performance, cost-effectiveness, and sustainability, nickel foam was selected as the current collector in this study [12].
For binder type study, visual inspection between electrode using binder PVDF (left-side petri dish) and PTFE (right-side petri dish) as shown in Figure 3 (c) initial immersion, and 3 (d) after 1 month. It showed minimal physical changes, indicating good structural integrity of the electrode [13]. These findings suggest that the chosen current collector and binder combination is stable under prolonged exposure to electrolyte, making it a suitable candidate for long-term use in supercapacitors and similar energy storage devices.

Meanwhile, Figure 3 (e) shows a condition of surface morphology of the Ni foam before and Figure 3 (f) after undergoing the experiment. The results showed minimal changes for electrode that coated with PTFE binder, indicating that the current collector remains stable when exposed to the electrolyte unlike the other sample which showed electrode peeling after 1-month immersion. This suggests PTFE binder can maintain its electrode's structure over time, making it suitable for long-term use in energy storage devices like supercapacitors or batteries. For this supercapacitor study, PTFE was selected as the binder due to its strong hydrophobic properties, which help ensure long-term durability and performance.

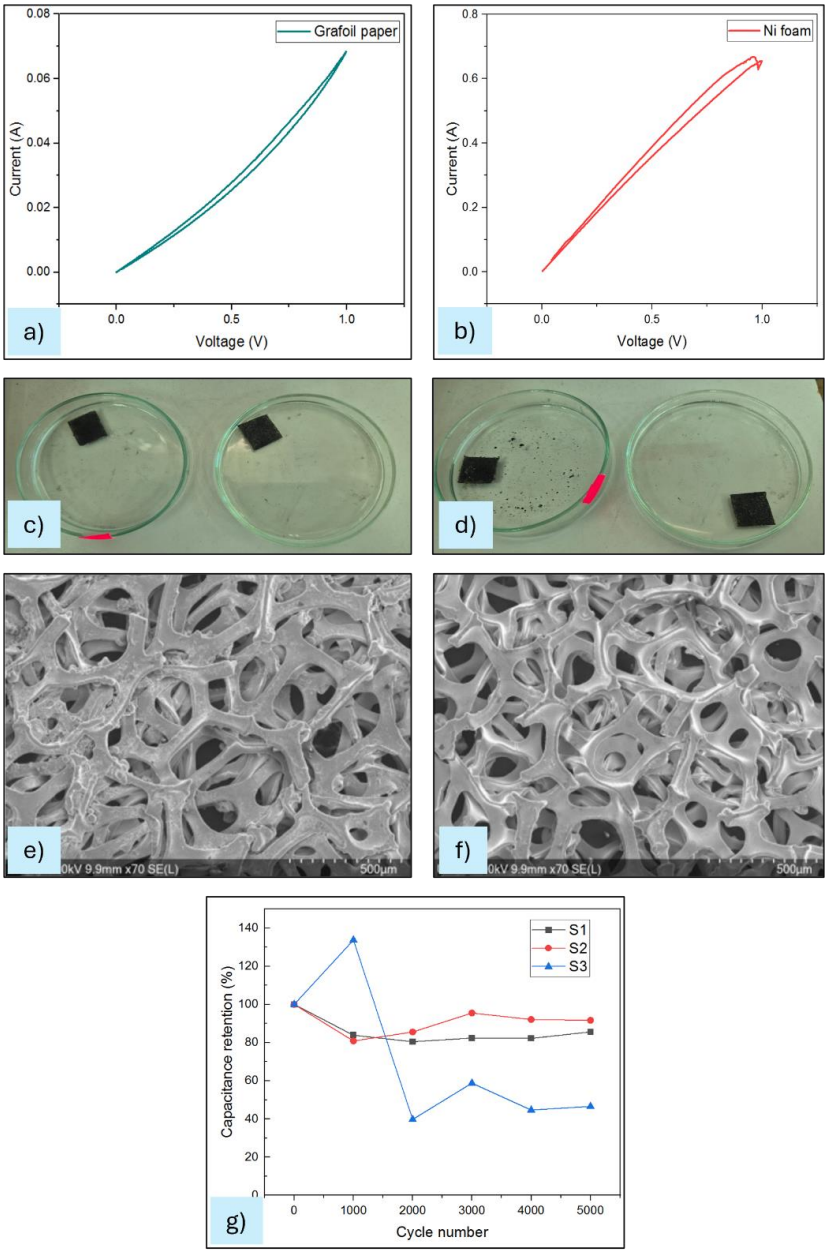

Figure 3: CV rates of (a) Grafoil paper and (b)Ni foam in 100 mVs^{-1}; Sample with different type of binders, (c) initial physical observation of electrode immersion in 6M KOH electrolyte [left PVDF, right: PTFE] (d) after one month of immersion; FESEM images of Ni foam (e) before and (f) after experiment in 70x magnification; (g) Cycling stability tested at applied current of 2 mA in 6M KOH electrolyte.

CV curves of MoS_2 electrodes with varying PTFE binder ratios, S1(5%), S2(10%), and S3(20%) showing near-rectangular shapes at higher scan rates, indicative of good EDLC behavior and low contact resistance. Among the tested samples, Sample 2 achieved the highest Csp value of 40.94 F g^{-1} at 10 mV s^{-1}, followed by Sample 1 (18.58 F g^{-1}) and Sample 3 (9.83 F g^{-1}). Further, cycling stability was assessed by repeating GCD tests for 5,000 cycles at 2 mA as shown in Figure 3 (g). Capacitance retention for Samples 1, 2, and 3 were 85%, 91%, and 46%, respectively, with Sample 2 (10 wt% PTFE) showing the highest stability [14]. To summarize, although 5 wt% and 20 wt% PTFE ratios showed good initial performance, the 10 wt% PTFE binder provided superior capacitance retention and stability. Therefore, this binder ratio was selected for fabricating the Ti_3C_2 MXene/MoS_2 hybrid electrode used in this study.

3.3 Electrochemical Performance MoS_2/Ti_3C_2 MXene Hybrid Supercapacitor Electrode

CV is a fundamental electrochemical technique used to evaluate specific capacitance by applying a cyclic potential scan within a defined voltage range and recording the current response [15, 16]. The shape and area of the CV curves provide insights into charge storage behavior, capacitive performance, and redox activity. Specific capacitance is determined from the curve area, with larger areas corresponding to higher charge storage capacity. Additionally, scan rate-dependent CV analysis offers information on ion diffusion and electrochemical kinetics, supporting the assessment of electrode suitability for supercapacitor applications [17].

Subsequently, the selected samples were subjected to further analysis. Figure 4 presents the CV curves and corresponding data for the Ti_3C_2 MXene/MoS_2 electrode tested in three different electrolytes: 6 M KOH, 1 M H_2SO_4, and 1 M Na_2SO_4 electrolyte. The results highlight the influence of electrolyte type on the electrode's electrochemical performance. Among the tested electrolytes, KOH demonstrated superior performance due to its high ionic conductivity and rapid ion diffusion, making it suitable for high-power supercapacitor applications. In contrast, Na_2SO_4 showed moderate conductivity, suggesting its

suitability for applications emphasizing long-term stability and durability. H_2SO_4 offered high conductivity, but its use requires careful assessment of material compatibility due to potential reactivity with the electrode.

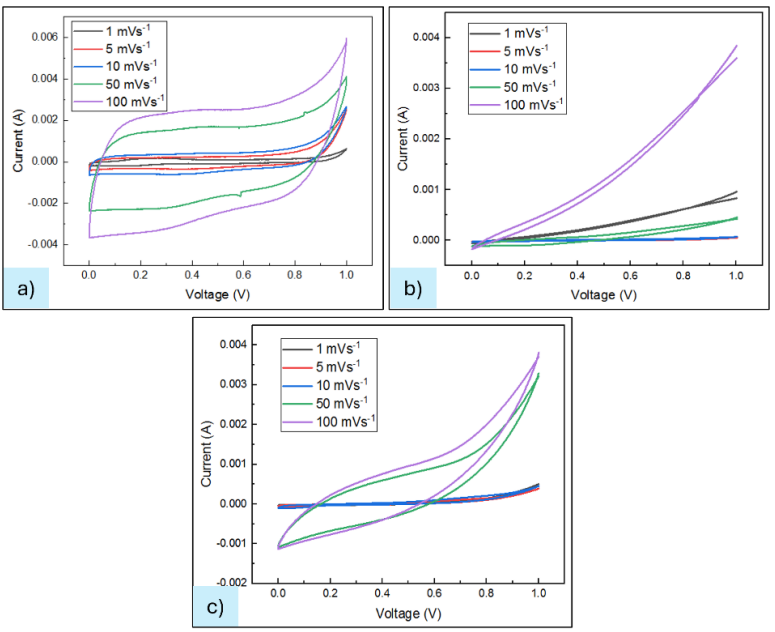

Figure 4: CV of the hybrid electrode in 3 different type or electrolytes; a) in 6M KOH, b) 1M H2SO4 and c) 1M Na2SO4

Table 3: Specific capacitance of the hybrid electrode in different electrolytes

Electrolyte	Active mass	Scan rates (mVs^{-1})	Area under the curve ($unit^2$)	Specific capacitance (Fg^{-1})
6M KOH	3.87	1	20.778	80.410
		5	51.222	39.645
		10	82.798	32.043
		50	300.98	23.300
		100	455.20	17.616
1M H_2SO_4	2.58	1	0.737	1.901
		5	1.017	0.528
		10	1.531	0.395
		50	7.692	0.400
		100	8.101	0.209
0.5M Na_2SO_4	2.81	1	1.369	3.847
		5	3.664	2.059
		10	5.742	1.614
		50	67.526	3.795
		100	81.001	2.276

The intercalation mechanism in KOH electrolyte involves the insertion of potassium ions (K^+) into the layered structure of MoS_2 or MoS_2/MXene composites. The high ionic conductivity of KOH facilitates rapid ion transport, which enhances the electrochemical performance of supercapacitors [18]. The incorporation of K^+ ions in hybrid heterostructures increases charge storage capacity by promoting electric double-layer formation at the electrode interface. This process improves overall capacitance while maintaining structural stability during cycling, thereby supporting long-term performance. For sulphuric acid electrolyte, it splits into sulfate (SO^{4-}) and hydrogen ions (H^+), and the larger ion concentrations are what give the electrochemical properties—specifically, its capacitance; bringing interactions take place between protons in the acidic solution and terminations on the surface of the hybrid electrodes [19].

On the other hand, sodium sulfate the other neutral medium for ion intercalation, primarily through Na^+ ions with high mobility that enable effective penetration into hybrid heterostructures. Its neutral nature also minimizes corrosion within the electrochemical system. Neutral electrolyte also mentioned to be having lower self-discharge compared to acidic- and alkaline-based electrolyte [20], noting the exploration towards slow and stable discharging ion transfer. The mechanisms of all electrolytes are illustrated in **Figure 5**.

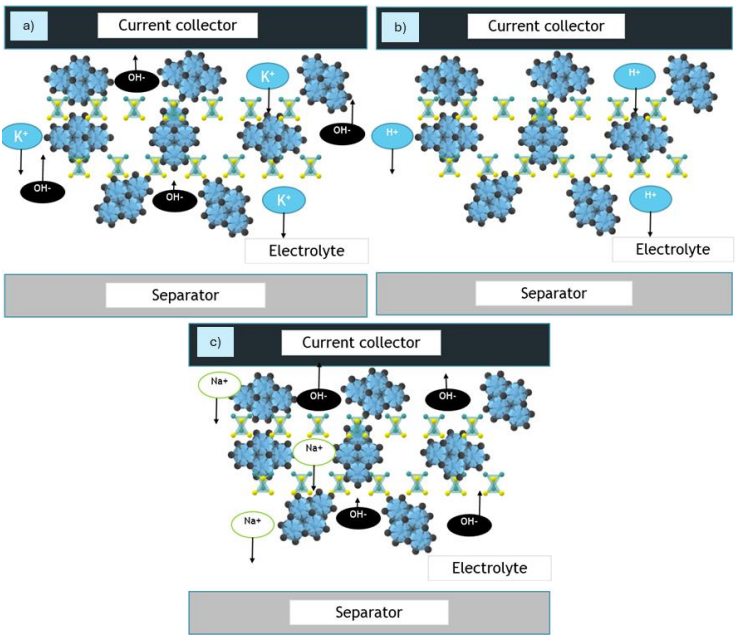

Figure 5: Electrolyte intercalation mechanism for 3 type or electrolytes; a) in 6M KOH, b) 1M H_2SO_4 and c) 1M Na_2SO_4

4.0 CONCLUSION

In this study, a hybrid electrode was successfully fabricated by combining MoS_2 and Ti_3C_2 MXene using a hydrothermal synthesis method. Three types of electrolytes were employed: three aqueous electrolytes (6 M KOH, 1 M H_2SO_4, and 0.5 M Na_2SO_4). The optimized composition was identified as 70% Ti_3C_2 MXene and 30% MoS_2, based on superior electrochemical performance. Structural characterization confirmed the successful synthesis of the hybrid material. XRD confirmed the crystalline nature of the heterostructure and the deposition of Ti_3C_2 MXene onto exfoliated MoS_2. FESEM revealed the characteristic layered morphology of Ti_3C_2 MXene, consistent with the removal of aluminum from Ti_3AlC_2. Electrochemical testing was conducted using CV and galvanostatic GCD. The hybrid electrode exhibited favorable energy and power densities, making it suitable for both symmetric and asymmetric supercapacitor applications. The triangular shape of the CV curves and the consistent performance across charge–discharge cycles confirm the capacitive behavior and efficient ion transport properties of the material. These findings suggest that the MXene/MoS_2 hybrid is a strong candidate for next-generation energy storage devices.

ACKNOWLEDGMENTS

The authors thank Faculty of Industrial and Manufacturing Technology and Engineering, Universiti Teknikal Malaysia Melaka.

AUTHOR CONTRIBUTIONS

MA Kosnan: Writing - Original Draft, Formal Analysis, Visualization MA Azam: Conceptualization, Supervision, Resources NE Safie: Writing- Reviewing and Editing RF Munawar: Data Curation, Methodology IS Othman: Writing- Reviewing and Editing JA Razak: Writing- Reviewing and Editing A Takasaki: Methodology MF Allim: Writing- Reviewing and Editing, Data curation MK Shabdin: Writing- Reviewing and Editing M Yassir: Resources

CONFLICTS OF INTEREST

The manuscript has not been published elsewhere and is not under consideration by other journals. All authors have approved the review, agree with its submission and declare no conflict of interest on the manuscript.

REFERENCES

[1] J. Qin, Z. Yang, F. Xing, L. Zhang, H. Zhang, and Z.-S. Wu, "Two-Dimensional Mesoporous Materials for Energy Storage and Conversion: Current Status, Chemical Synthesis and Challenging Perspectives," *Electrochemical Energy Reviews*, vol. 6, no. 1, 2023.

[2] Z. Wang and B. Mi, "Environmental Applications of 2D Molybdenum Disulfide (MoS_2) Nanosheets," *Environmental Science & Technology*, vol. 51, no. 15, pp. 8229–8244, 2017.

[3] R. Dhilip Kumar, S. Nagarani, V. Sethuraman, S. Andra, and V. Dhinakaran, "Investigations of conducting polymers, carbon materials, oxide and sulfide materials for supercapacitor applications: a review," *Chemical Papers*, vol. 76, no. 6, pp. 3371–3385, 2022.

[4] T. Bashir, S. Zhou, S. Yang, S.A. Ismail, T. Ali, H. Wang, J. Zhao and L. Gao,

"Progress in 3D-MXene Electrodes for Lithium/Sodium/Potassium/Magnesium/Zinc/Aluminum-Ion Batteries," *Electrochemical Energy Reviews*, vol. 6, no. 1, pp. 1-34, 2023.

[5] N. Jahan et al., "Structural, Morphological and Elemental Analysis of Selectively Etched and Exfoliated Ti3AlC2 MAX Phase," *Journal of Multidisciplinary Applied Natural Science*, vol. 1, no. 1, pp. 13–17,. 2021.

[6] H.Q. Wang, J.W. Wang, X.Z. Wang, X.H. Gao, G.C. Zhuang, J.B. Yang, H. Ren, "Dielectric properties and energy storage performance of PVDF-based composites with MoS_2@MXene nanofiller," *Chemical Engineering Journal,* vol. 437, no. 2, p. 135431, 2022.

[7] S. Alam, A. Jan, M.Z. Iqbal, I.S. Yahia, H.H. Hegazy, M.I. Saleem, "Unveiling the advancements in electrochemical performance of 2D transition metal dichalcogenides as an electrode material in asymmetric supercapacitors", *Materials Chemistry and Physics,* vol.334, p. 130444, 2025.

[8] Chandran M, Thomas A, Raveendran A, Vinoba M, Bhagiyalakshmi M, "MoS_2 confined MXene heterostructures as electrode material for energy storage application", *Journal of Energy Storage,* vol. 30, p. 101446, 2020.

[9] S Karmakar, A Mandal, NK Mani, R Sha, "Review: 2D MXenes based electrochemical sensors and supercapacitors for biomedical and energy storage applications", *Materials Chemistry and Physics*, vol. 343, p. 130974, 2025.

[10] E Pollack, Q Zhou, E Loni, K Agbakansi, A Majed, F Wang, A Soleymani, M Busse, M Naguib, X Lu, "Raman spectroscopy of 2D MoS_2 on Ti_3C_2 MXene: the substrate effect", *Nanoscale Advances,* vol. 7, no. 11, pp. 3456–3461, 2025.

[11] D.A. Bograchev, Y.M. Volfkovich, S. Martemianov, "Diagnostics of supercapacitors using cyclic voltammetry: modeling and experimental applications", *Journal of Electroanalytical Chemistry,* vol. 935, p. 117322, 2023.

[12] MS Ratsoma, BLO Poho, K Makgopa, K Raju, KD Modibane, CJ Jafta, KO Oyedotun, "Application of nickel foam in electrochemical systems: a review", *Journal of Electronic Materials,* vol. 52, pp. 2264–2291, 2023.

[13] D Choi, Y Lee, ZH Lin, S Cho, M Kim, CK Ao, S Soh, C Sohn, CK Jeong, J. Lee, "Recent advances in triboelectric nanogenerators: From technological progress to commercial applications", *ACS Nano,* vol. 17, no. 12, 11087–11219 (2023).

[14] L Zhang, T Xia, X Yuan, G Wang, Y Liu, X Yang, Q Ding, J Tang, H Li, Y Zhang**,** "Feasible approach to prepare 60%-purity metallic phase MoS_2 with high stability for superior supercapacitor performance", *Inorganic Chemistry Communications,* vol. 181, no. 1, p. 115171, 2025

[15] B. Kirubasankar, M. Narayanasamy, J. Yang, M. Han, W. Zhu, Y. Su, S. Angaiah, C. Yan, "Construction of heterogeneous 2D layered MoS_2/MXene nanohybrid anode material via surfactant-assisted interstratification

process and its synergetic effect for asymmetric supercapacitors", *Applied Surface Science,* vol. 516, p.146444, 2020.

[16] O Gharbi, MTT Tran, B Tribollet, M Turmine, V Vivier, "Revisiting cyclic voltammetry and electrochemical impedance spectroscopy analysis for capacitance measurements", *Electrochimica Acta,* vol. 343, p. 136109, 2020.

[17] S Yang, Y Li, Q Chen**.,** **"**Resolving electron transfer kinetics in porous electrodes via diffusion-less cyclic voltammetry", *Journal of Materials Chemistry A,* 9 pp. 14025–14031, 2021.

[18] S Lu, Y Song, K Guo, X Chen, J Xu, L Zhao, "Effect of aqueous electrolytes on the electrochemical behaviors of ordered mesoporous carbon composites after KOH activation as supercapacitor electrodes", *Journal of Electroanalytical Chemistry,* vol. 818, pp. 58–67, 2018.

[19] MA Anu, M Tomy, U Manimehala, TS Xavier, "Supercapacitor featuring $Ti_3C_2T_x$ MXene electrode: Nanoarchitectonics and electrochemical performances in aqueous and non-aqueous electrolytes", *Materials Research Bulletin,* vol. 173, p. 113315, 2025.

[20] W Zheng, J Halim, POÅ Persson, J Rosen, MW Barsoum. Effect of vacancies on the electrochemical behavior of Mo-based MXenes in aqueous supercapacitors. *Journal of Power Sources,* vol. 525, p. 231064, 2022.